

HD-A134 233

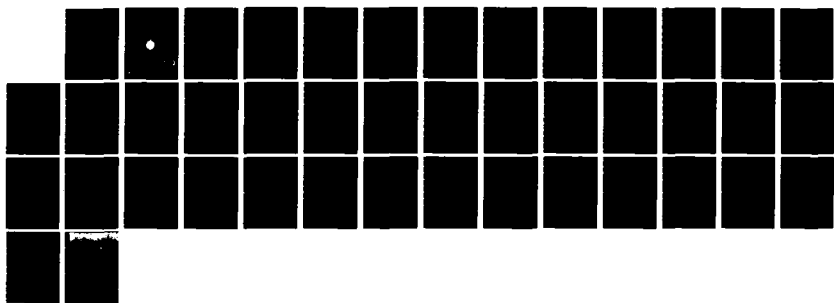
PROPELLER CAVITATION EFFECTS ON BROADBAND  
VESSEL-RADIATED ACOUSTIC SPECTRUM NAVAL ACADEMY  
ANNAPOLIS MD D N DIXON 20 JUN 83 USNA-TSPR-123

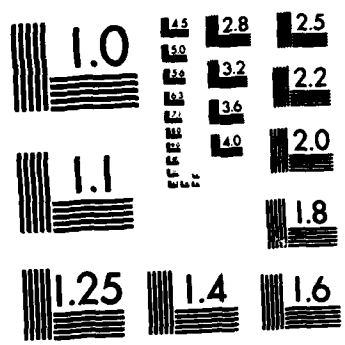
1/1

UNCLASSIFIED

F/G 20/1

NL





MICROCOPY RESOLUTION TEST CHART  
NATIONAL BUREAU OF STANDARDS-1963-A

AD-A134233

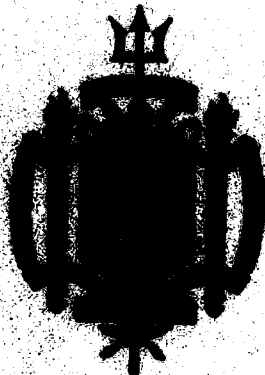
AD-A134233

A TRIDENT SCHOLAR  
PROJECT REPORT

NO. 123

23

PROPELLER CAVITATION EFFECTS ON BROADBAND  
VESSEL-RADIATED ACOUSTIC SPECTRA



UNITED STATES NAVAL ACADEMY  
ANNAPOLIS, MARYLAND

1983

This document has been approved for public  
release and sale; its distribution is unlimited.

DTIC  
ELECTED  
OCT 31 1983  
S D  
B

83 10 28 034

U.S.N.A. - Trident Scholar project report; no. 123 (1983)

"Propeller Cavitation Effects on Broadband  
Vessel-Radiated Acoustic Spectra"

A Trident Scholar Project Report

by

Midshipman 1/c Daniel N. Dixon '83

U. S. Naval Academy

Annapolis, Maryland

Supported (in part) by

Naval Sea Systems Command

R L Jernette Physics  
Advisor Department

Accepted for Trident Scholar Committee

Chair & Rec'd  
Chairman

June 20, 1983  
Date

DTIC  
ELECTED  
OCT 31 1983

B

A

## ABSTRACT

To gain an understanding of ambient noise in the oceans today, the characteristics of merchant vessel acoustic spectra must be determined. Presently, it is believed that the major source of acoustic intensity emanating from a merchant is propeller noise. Experimental data must be gathered to verify if propeller noise is the dominating contributor to the far field radiated merchant vessel spectrum.

Data was gathered from a stationary vessel whose propellers are cavitating to determine exactly how much of the far field spectrum was propeller dominated. Considerations such as propagation delay and multi-path effects had to be dealt with prior to the processing procedure. Digital signal processing techniques along with the coherence function were applied to the gathered data. The resulting coherence values for frequencies of interest to Navy sonar systems (0-500 Hz) were studied and compared to the corresponding signal-to-noise level in the far field spectrum. The coherence accurately displays that, contrary to present belief, propeller cavitation is not the dominant source of merchant vessel acoustic power in the far field over the entire frequency band of interest.

Classification	
Approved for:	
NTIS GEN ID	
DTIC FILE	
Unannounced	
Justification	
By _____	
Distribution/	
Availability Codes	
Dist	Aveit and/or Special
A-1	



#### ACKNOWLEDGEMENTS

It would take many pages to thank all the wonderful people who have assisted me in the completion of this project. I would like to extend a general thank you, though, to all the professors, technicians and secretaries who provided a much-needed hand throughout the year. I extend my special appreciation to Prof. Bob Jennette whose all-encompassing expertise and skillful prodding provided the necessary impetus to keep the project moving as well as interesting. Not only did Prof. Jennette open my eyes to the field of underwater acoustics but he also exposed me to the workings of Navy research outside the Academy. The valuable experience I gained during our engagements in Crystal City, will most likely carry through the rest of my career. In this light, I would like to thank Capt. Henifin (Director, Research and Technology Office, Naval Sea Systems Command), whose interest and support were invaluable. In addition, a special thanks to LT. John Tandy for his helpful advise and keen wit which always kept things in perspective for me. Furthermore, the crew of YP654 should be commended for their patient waiting and eager assistance during the data gathering periods. Finally, I would like to thank Pat Kelly and Brenda Davis for their cheerful and gracious support throughout the year.

## TABLE OF CONTENTS

<b>Abstract .....</b>	1
<b>Acknowledgements .....</b>	2
<b>Table of Contents .....</b>	3
<b>Index to Figures .....</b>	4
<b>I. Introduction .....</b>	5
<b>II. The Coherence Function .....</b>	8
<b>III. The Effects of Time Delay on the Coherence Function .....</b>	11
<b>IV. Digital Time Windows .....</b>	13
<b>V. The Effect of Multi-Path on the Coherence Function .....</b>	15
<b>VI. Summary of Theoretical Analysis .....</b>	17
<b>VII. The Experiment Itself .....</b>	19
<b>VIII. Determining the Maximum Expected Coherence .....</b>	24
<b>IX. Coherence Function Characteristics .....</b>	30
<b>X. Summary of Results .....</b>	35
<b>References .....</b>	37

**INDEX TO FIGURES**

<b>Figure</b>	<b>Page</b>
1 Experimental Procedure .....	6
2 Power Spectrum- Far Field Ambient .....	20
3 Power Spectrum- Far Field .....	21
4 Coherence Function (with YP) .....	23
5 Power Spectra- Tone Generator .....	26
6 Coherence Function- Tone Generator .....	27
7 Coherence Function (Far vs. Near Field Ambient) .....	29

..

## PROPELLER CAVITATION EFFECTS ON THE VESSEL RADIATED ACOUSTIC SPECTRA

### I. INTRODUCTION.

Recently, acousticians<sup>1,2,3</sup> have tried to discover a feasible technique to measure the prominent source of acoustic power emanating from a merchant vessel. It is believed that propeller cavitation is the major contributor to merchant vessel radiated noise, but the fraction of the total power which actually comes from this cavitation is not presently known. The objective of this research effort is to measure this percentage.

Many new mathematical algorithms are available to the experimenter with the recent development of real time spectrum analyzers which solve many of the inherent problems previously encountered in underwater data gathering and processing. Using these advanced signal processing devices, the coherence function appears to be the proper mathematical relation to measure the effect propeller cavitation has on the total acoustic signature.

Once the mathematical and signal processing techniques had been established, a feasible experimental design was developed. The experimental setup was designed with easily accessible resources to make the process repeatable, and also to allow for relatively unlimited static data gathering. Vessel data was taken at two locations: in the near field of the propellers, and in the far field of the entire vessel (see figure 1). The near field signal is totally dominated by propeller noise, and the far field signal is equidistant from all noise sources of the vessel. The vessel was an 80 foot displacement craft having four diesel engines, a 60

# EXPERIMENTAL PROCEDURE

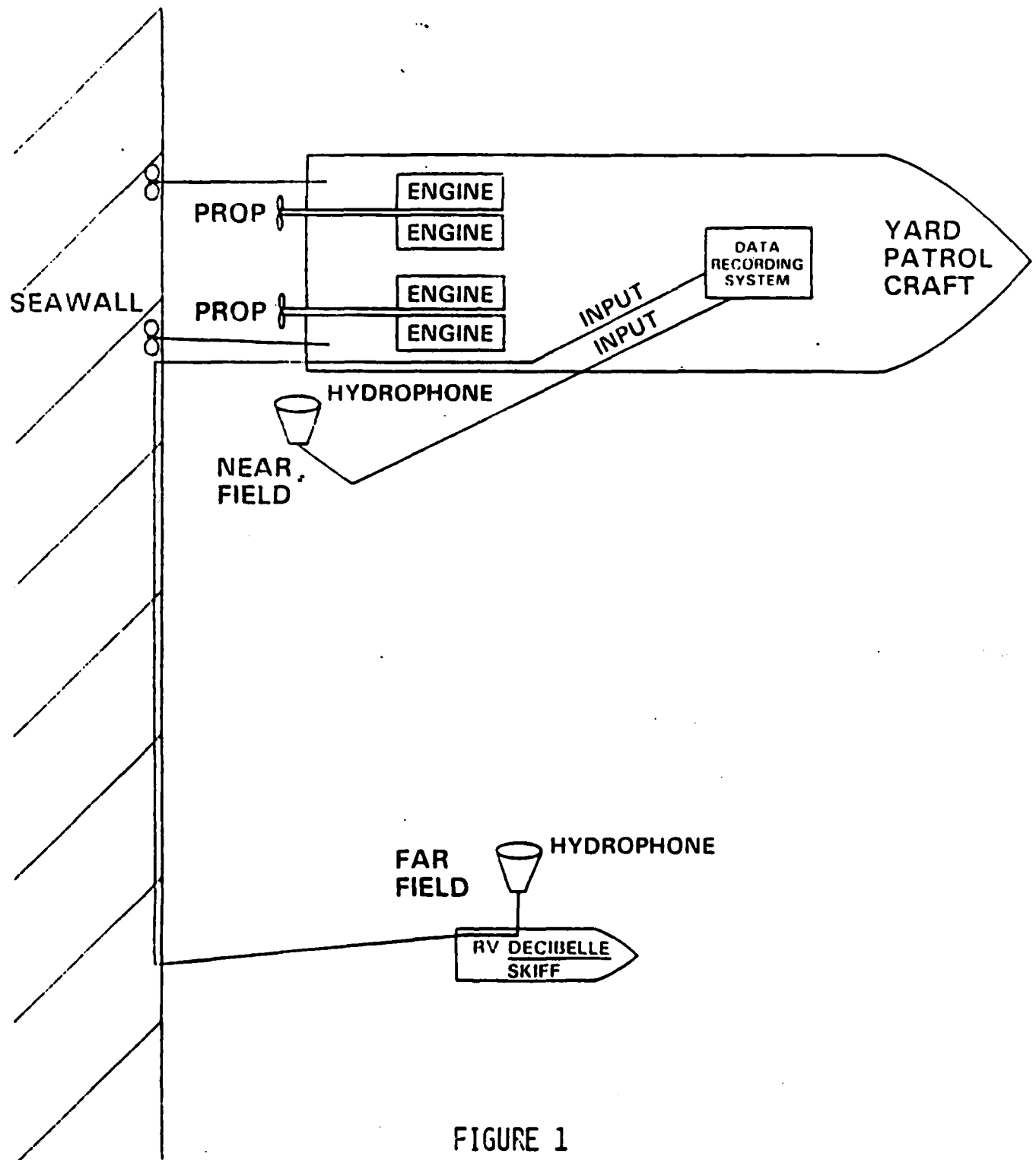


FIGURE 1

Hz generator, and twin three-foot diameter propellers. Having these characteristics as well as propellers which are known to cavitate at low speeds, this craft is assumed to be acoustically similar to a merchant vessel. The normal use of this boat is to train midshipmen in seamanship skills and has the designation of Yard Patrol Craft (YP). The YP will push against a seawall allowing for the procurement of sound readings on a cavitating, immobile vessel. Thus, with such an experimental layout, almost unlimited data may be gathered and recorded for later signal processing.

A theoretical investigation was initiated to show that the experiment is relevant to vessels in the ocean where the depth is essentially infinite. An analysis was undertaken to determine whether a mathematical function could be used to essentially eliminate the multi-path and time delay problems inherent with a shallow water environment. Looking ahead, the coherence function proves to be the ideal algorithm to determine the effect propeller cavitation has on the broadband merchant vessel radiated acoustic spectra.

The procurement of acoustic data such as that described above is of critical importance to the Navy today. Presently, underwater acoustic thresholds are limited by the amount of the ambient noise intensity present at the hydrophone or detection site. Merchant vessel traffic is known to be the major source of ambient noise in the ocean today. Therefore, the more information gained on the merchant vessel acoustic spectra, the better ambient noise is understood, and hopefully the Navy can increase its acoustic thresholds and detect targets from greater distances. Because of the major threat presented by hostile submarines, underwater acoustic research for the Navy will always be given a high priority.

## II. THE COHERENCE FUNCTION.

In order to process the data in a precise and expedient manner, a mathematical algorithm had to be found or developed which can be handled digitally and also yields the desired output. Furthermore, the mathematics must be able to account for the many unique qualities involved with the acoustic data. The important qualities include the multiple paths of a water environment and the finite propagation time of sound traveling a distance in the water. Herein lies the major complexity involved with underwater acoustic research, molding the mathematics to the unique requirements of the research. After investigating many mathematical functions it was determined that the coherence function satisfies all the requirements necessary to yield the appropriate results.

It can be shown that the coherence function measures the fraction of the total power in the far field signal which was caused by power present in the near field signal. In the case of the YP, the near field signal will be attained from a hydrophone close to the YP. It is necessary for the near field hydrophone to be very near the propeller because this entire signal must be assumed to be propeller dominated for the purposes of this analysis. The coherence function is defined as:

$$\gamma^2 = \frac{|\langle G_{xy} \rangle|^2}{\langle G_{xx} \rangle \langle G_{yy} \rangle}$$

where  $G_{xy}$  is the cross power spectrum, and  $G_{xx}$  and  $G_{yy}$  are simply power spectral densities. The power is defined as:

$$G_{xx} = X(f)X^*(f)$$

for a given signal  $x(t)$ , and where  $X(f)$  is the Fourier transform of  $x(t)$ .

In the experimental set-up:

Near Field Signal:  $x(t) = \text{propeller noise}$

Far Field Signal :  $y(t) = ax(t) + n(t) = \text{propeller noise} + \text{other noise}$

where  $a = \text{propagation constant}$

Applying the Fourier transform:

$$x(t) \rightarrow X(f) = R_x e^{i\phi_x}$$

$$y(t) \rightarrow Y(f) = aR_x e^{i\phi_x} + R_n e^{i\phi_n}$$

Proceeding to the coherence function:

$$G_{xy} = X(f)Y^*(f) = (R_x e^{i\phi_x})(aR_x e^{i\phi_x} + R_n e^{i\phi_n})^*$$

$$G_{xy} = aR_x R_x^* + R_x R_n^* e^{i(\phi_x - \phi_n)}$$

$$\langle G_{xy} \rangle = aR_x R_x^*$$

In the averaging process inherent in the coherence function all uncorrelated terms go to zero. The detailed reasoning behind this reduction is covered in the time delay section.

Going on to the denominator of the coherence function:

$$G_{xx} = X(f)X^*(f) = (R_x e^{i\phi_x})(R_x e^{i\phi_x})^*$$

$$\langle G_{xx} \rangle = R_x R_x^*$$

$$G_{yy} = Y(f)Y^*(f) = (aR_x e^{i\phi_x} + R_n e^{i\phi_n})(aR_x e^{i\phi_x} + R_n e^{i\phi_n})^*$$

$$\langle G_{yy} \rangle = a^2 R_x R_x^* + R_n R_n^*$$

again the uncorrelated terms go to zero when averaged.

Finally,

$$\gamma^2 = \frac{|\langle G_{xy} \rangle|^2}{\langle G_{xx} \rangle \langle G_{yy} \rangle}$$

$$\gamma^2 = \frac{|\alpha R_x R_x^*|^2}{(R_x R_x^*)(\alpha^2 R_x R_x^* + R_n R_n^*)}$$

$$\gamma^2 = \frac{\alpha^2 R_x R_x^*}{\alpha^2 R_x R_x^* + R_n R_n^*}$$

$$\gamma^2 = \frac{\text{INPUT POWER}}{\text{OUTPUT POWER}}$$

where the output power consists of input power and noise power.

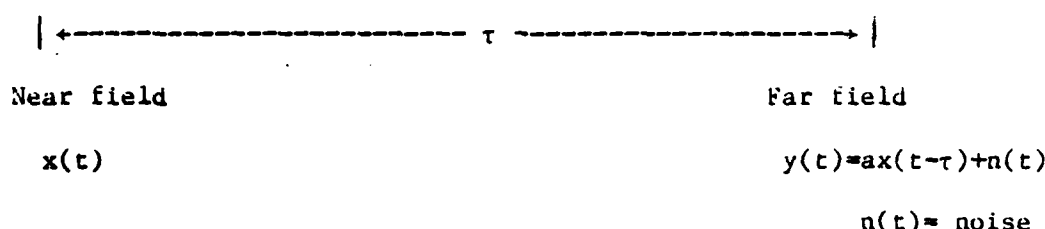
Therefore, the above ratio is exactly what is needed to discover just how much of the far field power is caused by propeller cavitation.

All the mathematical operations necessary for application of the coherence function are performed digitally using state-of-the-art signal processing techniques. The recorded time series are digitally sampled and separated into time windows such that the Nyquist Theorem is satisfied. The Nyquist Theorem states that sampling must be performed at twice the highest frequency which is contained in the signal.<sup>4</sup> These discrete samples are then changed from the time domain to the frequency domain via a Fast Fourier transform algorithm(FFT). This Fourier transform technique yields 512 discrete frequency values across the desired frequency range (0-500 Hz). Finally, these frequency values are multiplied, conjugated and divided as required by the coherence function to yield the proper

result. This process is carried out for every time window. The duration of each window is approximately 0.8 seconds. Consequently, the speed of computation is of utmost importance in order not to lose any information from the incoming time series.

### III. THE EFFECT OF TIME DELAY ON THE COHERENCE FUNCTION.

From Figure 1 it can be seen that the signal received at the near field will not correspond exactly to the signal received at the same time in the far field. Simply stated, it takes a finite length of time for the signal in the near field to propagate to the far field in the underwater environment. The question to be dealt with is whether this time delay will limit the effectiveness of the coherence function. Incorporating the time delay into the signal looks like this:



Time delay,  $\tau$ , is the time it takes the signal,  $x(t)$ , to travel through the water to the far field. In this specific case assuming a speed of propagation of 1500 m/sec.

$$t = \frac{100 \text{ meters}}{1500 \text{ meters/second}} = 0.0667 \text{ seconds}$$

Applying the Fourier transform to the signals:

$$x(t) \rightarrow X(f) = R_x e^{i\phi_x}$$

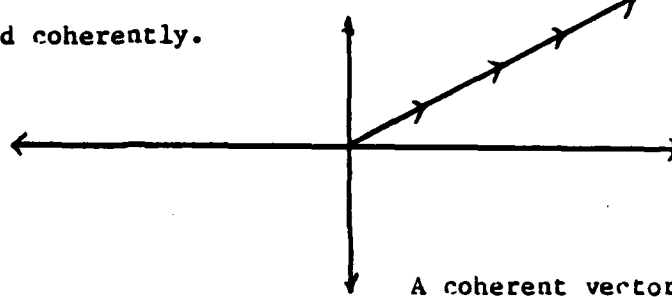
Proceeding to the definition of the coherence function once again, the numerator reduces to:

$$G_{xy} = X(f)Y^*(f) = (R_x e^{i\phi_x}) (a R_x e^{i\phi_x - i\omega\tau} + R_n e^{i\phi_n})^*$$

$$G_{xy} = a R_x R_x^* e^{i\omega\tau} + R_x R_n^* e^{i(\phi_x - \phi_n)}$$

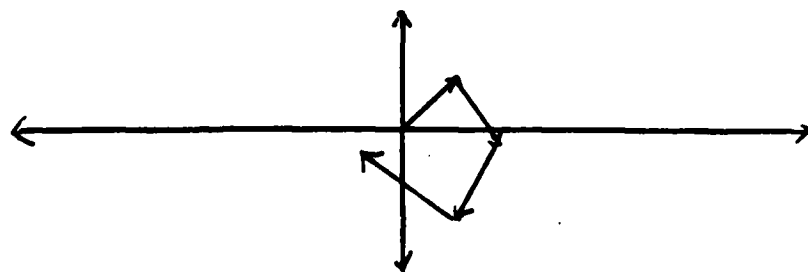
Considering each term separately as vectors in phase space:

$a R_x R_x^* e^{i\omega\tau}$  - always has the same phase,  $\omega\tau$ , so when averaged the vectors tend to add coherently.



A coherent vector sum.

$R_x R_n^* e^{i(\phi_x - \phi_n)}$  - since  $x$  and  $n$  are independent processes, the phases of the vectors vary randomly over the average, and hence the term is insignificant when compared to the first term of the numerator.



A random vector sum.

Herein lies the explanation of why the averaging process within the coherence function is so helpful in this application. Only the vectors which sum coherently are significant in the coherence measure, and these same vectors represent the coherent power in the far field.

The denominator of the coherence is unaffected by the time delay because the cross power spectrum of the same signal,  $G_{xx}$  or  $G_{yy}$ , negates the phase difference. In the average, the vectors representing both  $G_{xx}$  and  $G_{yy}$  have the same relative phase difference, and therefore tend to sum coherently.

$$\langle G_{xx} \rangle = \langle X(f)X^*(f) \rangle = R_x R_x^*$$

$$\langle G_{yy} \rangle = \langle Y(f)Y^*(f) \rangle = a^2 R_x R_x^* + R_n R_n^*$$

Cross terms are incoherent and go to zero when averaged as described earlier:

$$\langle G_{xx} \rangle \langle G_{yy} \rangle = (R_x R_x^*) (a^2 R_x R_x^* + R_n R_n^*)$$

Therefore, the coherence now looks like:

$$\gamma^2 = \frac{|aR_x R_x^* e^{i\omega t}|^2}{(R_x R_x^*)(a^2 R_x R_x^* + R_n R_n^*)} = \frac{a^2 R_x R_x^*}{a^2 R_x R_x^* + R_n R_n^*}$$

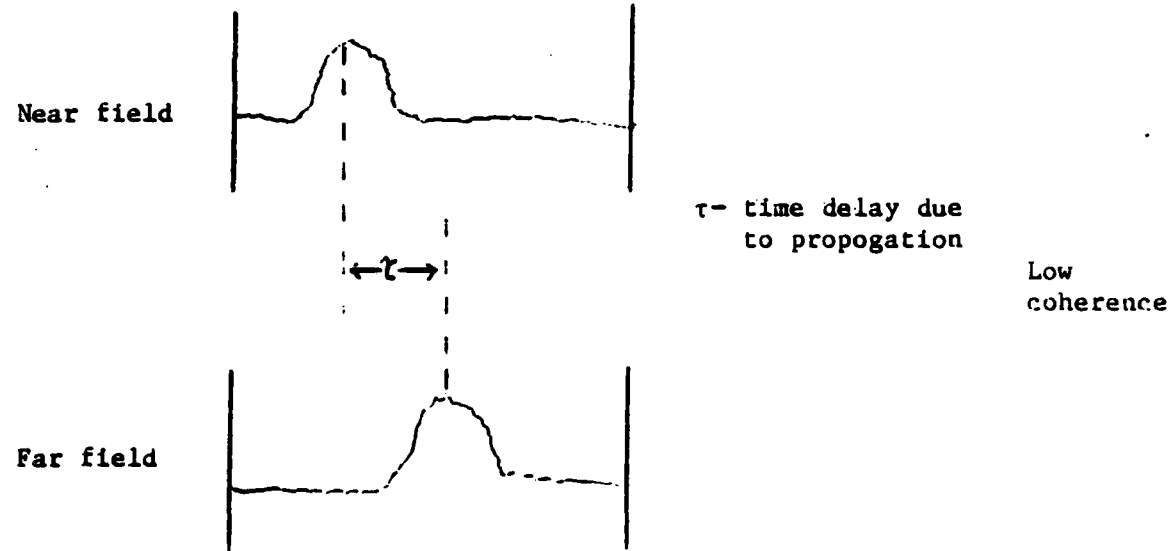
$$\gamma^2 = \frac{\text{INPUT POWER}}{\text{INPUT POWER} + \text{NOISE POWER}} = \frac{\text{INPUT POWER}}{\text{OUTPUT POWER}}$$

Once again the desired proportion of the output power caused by input power in the far field is obtained. Consequently, the time delay does not limit the effectiveness of the digitally processed coherence function.

#### IV. DIGITAL TIME WINDOWS.

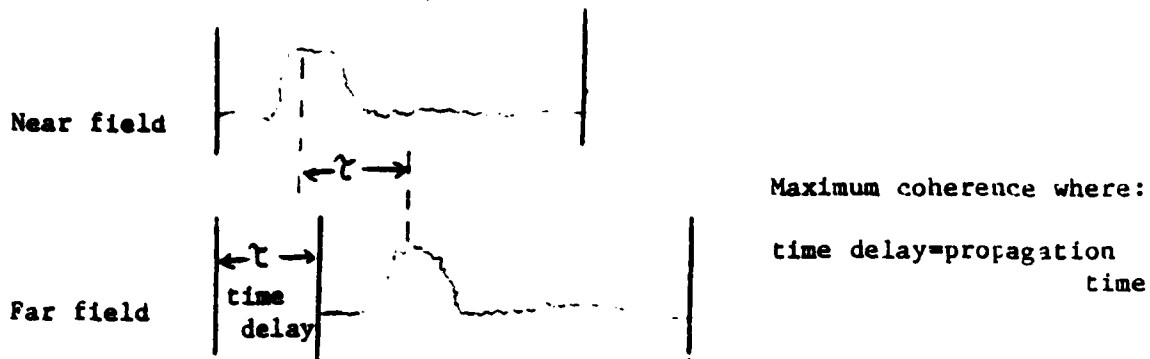
A major problem involved in the digital processing of the time delayed data is the adjustment of the sampling windows to get the desired "overlap" of the two time series. The reason this is important lies in the fact that both the near and far field signals are recorded simulta-

neously on an analog tape recorder. When the signal processor digitally samples this recording it performs all its computations with these parallel windows. In this experiment, a faulty coherence measure would be gained because the far field signal of interest does not run contiguously with the corresponding near field signal. Even though the propagation time is so small, some sort of digital delay must be implemented to obtain an exact coherence measure. In the frequency band of interest for this experiment, 0-500 Hz, the propagation time of approximately 0.07 seconds accounts for only 10 percent of the 0.8 second digital time window. A typical digital time window display with insufficient time delay would look like this:



As mentioned earlier, the entire signal in the near field of the propeller is considered to be the desired cavitation noise. Therefore, all of the far field time window which is not overlapped with the propeller noise signal emitted in the near field is considered incoherent noise. The less the amount of overlap the more inaccurate the measure of coherent

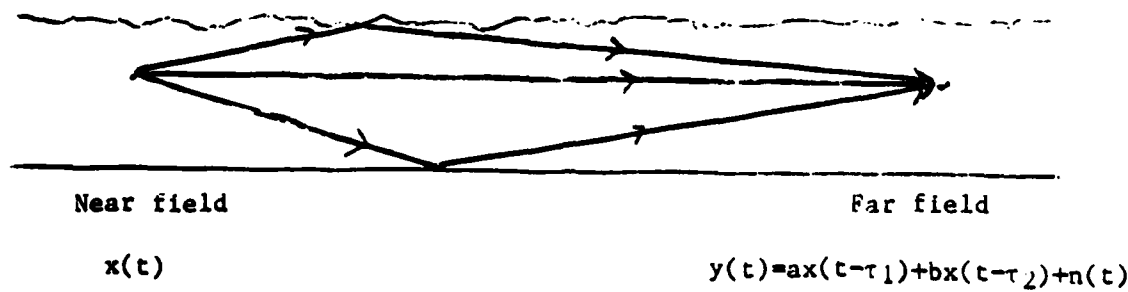
power in the far field. Fortunately, the signal processor contains a built-in digital time delay function which allows for the adjustment of the time windows for maximum overlap. The signal processor actually samples the near field signal and then waits 0.07 seconds, the programmed time, before sampling the far field signal:



Thus, the properties of digital time windows allow for the manipulation of the gathered data in order to ensure that the derived results are accurate.

#### V. THE EFFECT OF MULTI-PATH ON THE COHERENCE FUNCTION.

A final theoretical determination must be undertaken to see if the coherence function is adversely affected by the shallow water, multi-path environment present at the experimental site. The true question being posed here is, can the more easily used shallow water environment correctly represent the deep water environment of interest to sonar acousticians. Pictorially the multi-path situation looks like:



Where  $\tau_1$  and  $\tau_2$  are the two propagation times for the different paths.

Again using the Fourier transform (the spectrum uses the Fast Fourier transform, FFT):

$$x(t) \rightarrow X(f) = R_x e^{i\phi_x}$$

$$y(t) \rightarrow Y(f) = aR_x e^{i\phi_x - i\omega\tau_1} + bR_x e^{i\phi_x - i\omega\tau_2} + R_n e^{i\phi_n}$$

a and b are again propagation factors.

Applying these frequency spectrums to the coherence function, the numerator becomes:

$$G_{xy} = X(f)Y^*(f) = (R_x e^{i\phi_x})(aR_x e^{i\phi_x - i\omega\tau_1} + bR_x e^{i\phi_x - i\omega\tau_2} + R_n e^{i\phi_n})^*$$

$$G_{xy} = aR_x R_x^* e^{i\omega\tau_1} + bR_x R_x^* e^{i\omega\tau_2} + R_x R_n^* e^{i(\phi_x - \phi_n)}$$

The  $R_x R_n^*$  term goes to zero as the average is taken, this vector is random, whereas the other vector,  $R_x R_x^*$ , adds coherently in the average, so:

$$\langle G_{xy} \rangle = aR_x R_x^* e^{i\omega\tau_1} + bR_x R_x^* e^{i\omega\tau_2}$$

Continuing on with the numerator,

$$|\langle G_{xy} \rangle|^2 = (aR_x R_x^* e^{i\omega\tau_1} + bR_x R_x^* e^{i\omega\tau_2})(aR_x R_x^* e^{i\omega\tau_1} + bR_x R_x^* e^{i\omega\tau_2})^*$$

$$|\langle G_{xy} \rangle|^2 = (aR_x R_x^*)^2 + (bR_x R_x^*)^2 + ab(R_x R_x^*)^2 (e^{i\omega(\tau_1 - \tau_2)} + e^{i\omega(\tau_2 - \tau_1)})$$

$$|\langle G_{xy} \rangle|^2 = (aR_x R_x^*)^2 + (bR_x R_x^*)^2 + 2ab(R_x R_x^*) \cos(\omega\Delta\tau)$$

where  $\Delta\tau = \tau_1 - \tau_2$

The denominator becomes:

$$\langle G_{xx} \rangle = X(f)X^*(f) = R_x R_x^*$$

$$\langle G_{yy} \rangle = a^2 R_x R_x^* + b^2 R_x R_x^* + ab R_x R_x^* \cos(\omega \Delta \tau) + R_n R_n^*$$

Once again the cross terms,  $R_x R_n$ , are neglected in the averaging process.

Finally, the denominator becomes:

$$\langle G_{xx} \rangle \langle G_{yy} \rangle = R_x R_x^* (a^2 R_x R_x^* + b^2 R_x R_x^* + ab R_x R_x^* (2 \cos(\omega \Delta \tau)) + R_n R_n^*)$$

The coherence is:

$$\gamma^2 = \frac{a^2 R_x R_x^* + b^2 R_x R_x^* + 2ab R_x R_x^* \cos(\omega \Delta \tau)}{a^2 R_x R_x^* + b^2 R_x R_x^* + 2ab R_x R_x^* \cos(\omega \Delta \tau) + R_n R_n^*}$$

$$\gamma^2 = \frac{\text{INPUT POWER}}{\text{INPUT POWER} + \text{NOISE POWER}} = \frac{\text{INPUT POWER}}{\text{OUTPUT POWER}}$$

Thus, the multi-path environment does not represent a problem in determining the coherence value because the desired ratio of input power to output power is again obtained. Although, the multi-path problem is much more prominent in a shallow water environment, the ocean also portrays multi-path characteristics. Acoustic power may propagate via many differing paths such as convergence zones and the shallow waveguides above the thermal layer.

## VI. SUMMARY OF THEORETICAL ANALYSIS.

After a very general mathematical analysis of the problems associated with digitally applying data from a time delayed, multi-path environment,

the coherence function appears to be the most robust operation available for obtaining the desired ratio. Two unique qualities inherent in the coherence function which make it very useful in this specific application are the averaging process and the frequency dependence. The averages taken within the function basically integrate out the cross terms which are uncorrelated. The spectrum analyzer also can be adjusted to take different numbers of averages to gain a quicker (fewer averages) or more accurate (more averages) result depending on the requirements of the experiment. When more averages are taken the phase random vectors become more insignificant and the coherent vectors are overwhelming dominant. The high degree of precision desired necessitates the long period of data gathering which is incorporated into the experimental design.

The narrow-band frequency dependent characteristics of the coherence function are actually the underlying principles which allow for its application under the specific requirements of this experiment. When operating in the frequency domain, any dominant tonal qualities will only affect a small frequency bin, whereas in the time domain any strong tone would mask any truly useful information. Because of the large amount of energy localized at 60 Hz at the experimental site, a function which operates in the frequency domain is a necessity; that is the 60 Hz and harmonics would tend to dominate any broadband measure. A coherence value is computed within the spectrum analyzer for each of the 512 frequency bins. Thus, any frequency dependence in the propagation time or the multi-path characteristics would be treated on a frequency by frequency basis. Other time-dependent mathematical functions, such as the cross correlation function, would not reveal any frequency dependent signal characteristics.

Therefore, the coherence function was the mathematical operation chosen to describe the proportion of broadband merchant radiated noise which is caused by propeller cavitation.

## VII. THE EXPERIMENT ITSELF.

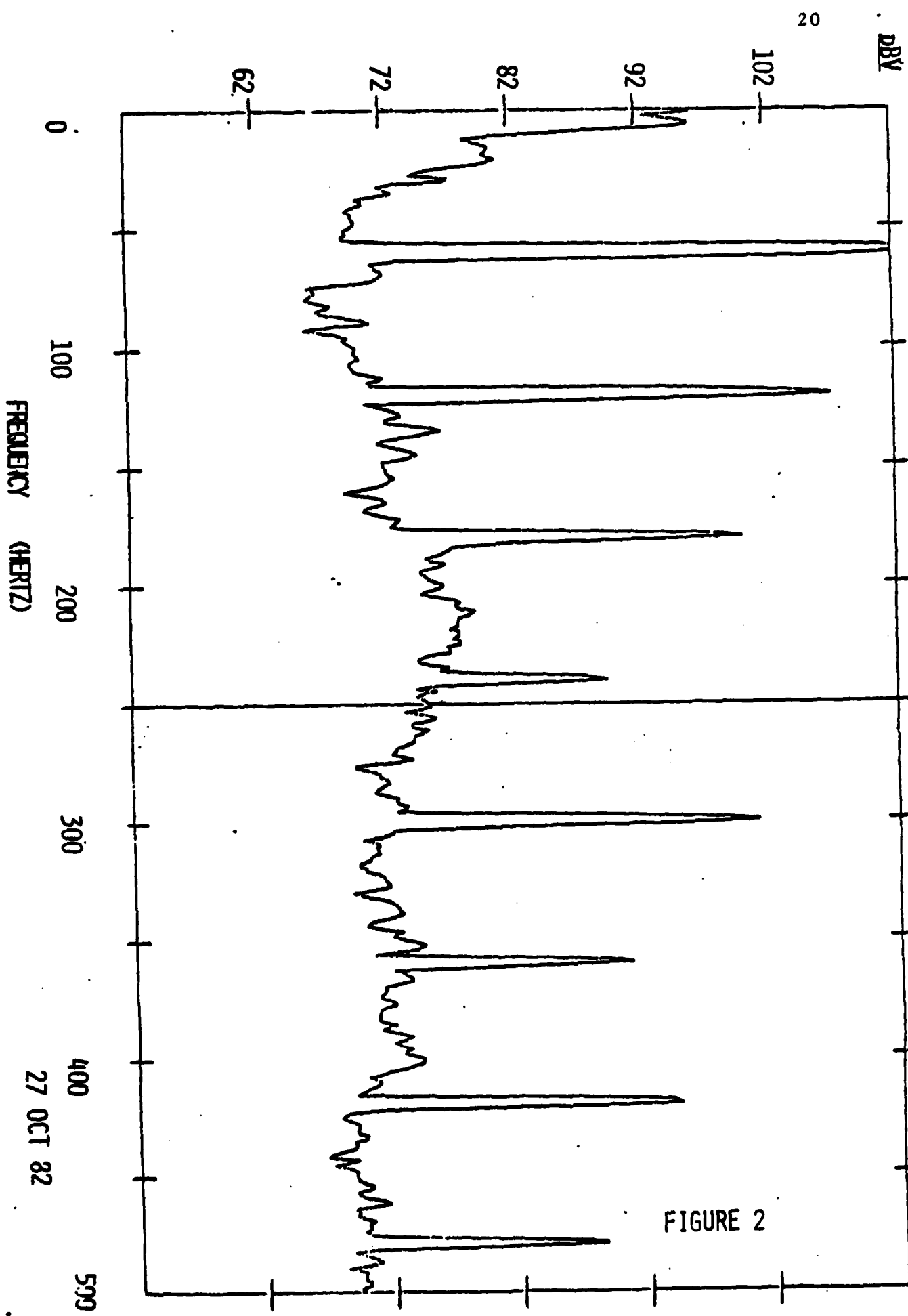
Data was gathered as described in the introduction for approximately twenty minutes at various shaft speeds. The near field hydrophone was kept within five feet of the propeller at all times, while the far field hydrophone was deployed approximately 350 feet from the vessel. The 350 foot distance allows for all sources of acoustic intensity emanating from the 80 foot YP to be considered as a point source of radiation. Ambient noise level readings from the far field hydrophone (figure 2) show that the 60 Hz tone and its harmonics dominate the ambient noise in the Severn River. This abundance of 60 Hz power is expected in the Severn because of the many power and communication lines along the bottom of the river. The remainder of the ambient noise spectrum is "bumpy-white" or Gaussian, as it would be in the ocean.

Figure 3 displays the signal-to-noise ratio created by the cavitating YP's acoustic spectrum in the far field. As can be seen from the figure, the signal emanating from the YP was predominantly over the ambient noise in the 120-300 Hz range. The remainder of the far field spectrum with the YP operating had no perceptible difference from the ambient levels in the 0-500 Hz range. During the data gathering process, a large amount of cavitation was visible from the stern of the YP. To verify whether this cavitation was truly the dominating source of the acoustic intensity received in the far field, the coherence function was applied to the near and far field signals. Figure 4 displays the coherence function from

POWER SPECTRUM - FAR FIELD AMBIENT

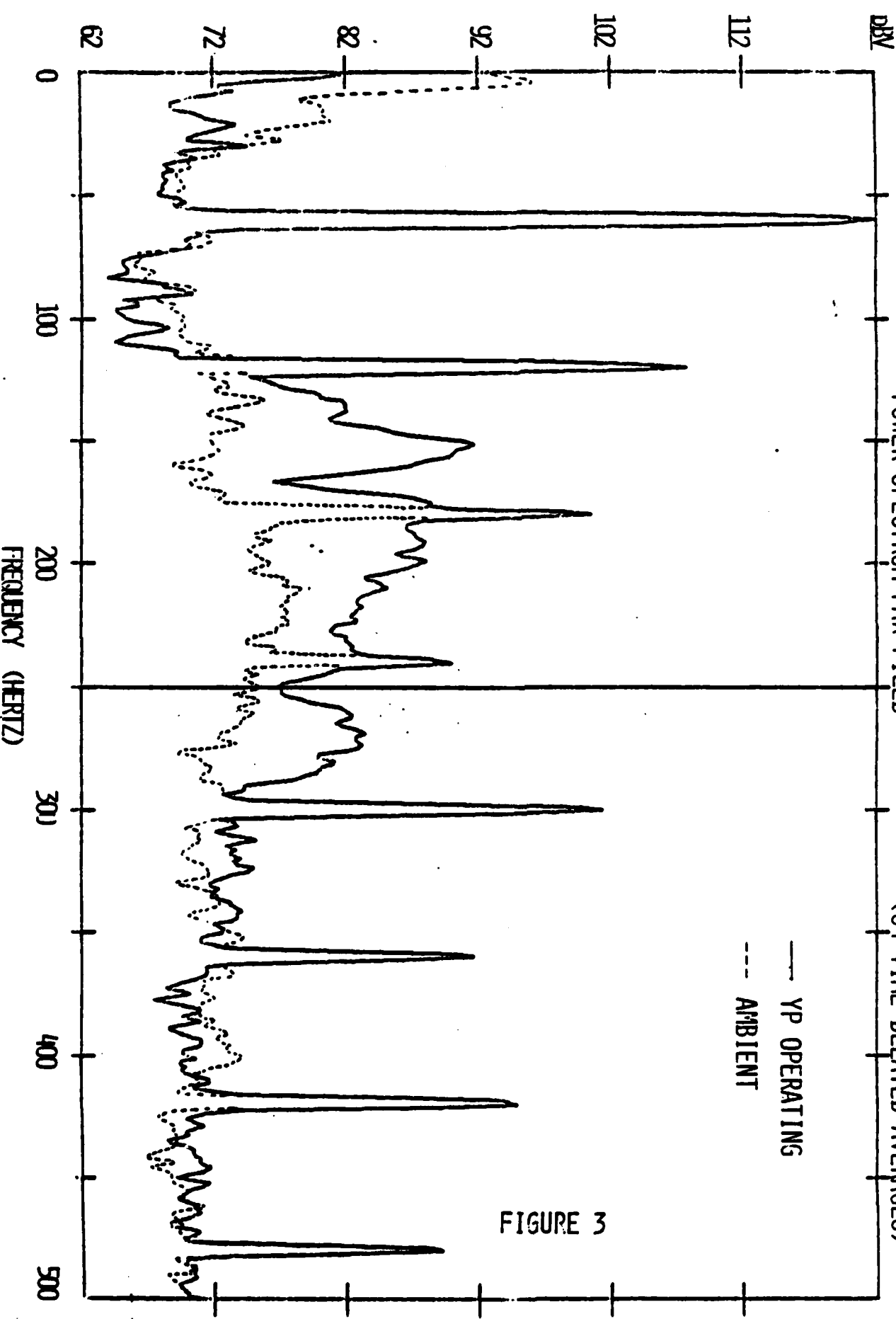
(32 AVERAGES)

FIGURE 2



## POWER SPECTRUM-FAR FIELD

(64 TIME-DELAYED AVERAGES)



0-500 Hz, 64 time-delayed spectral frames were averaged to produce an accurate representation. The 64 averages provide a very high confidence limit of approximately 90 percent which simply indicates that all phase and magnitude information will be accurate to within 10 percent. The time-delayed signal accounts for the time for the signal to propagate from the near field to the far field.

As expected, the coherence values in the 120-300 Hz range were much higher when compared to the other frequencies. These high coherence values verify that a high proportion of the far field intensity at these frequencies was caused by propeller cavitation. Because propeller cavitation is a modulated broadband Gaussian phenomenon, the coherence values in the region where good signal-to-noise existed are expected to be flat (constant) and not contain all the peaks and valleys as in figure 4. Of note is the fact that many of these peaks and valleys in the region of interest, 120-300 Hz, correspond to frequencies where there were either high or low signal-to-noise levels in the far field (figure 3). Later, it will be discussed how this "jaggedness" in the coherence cannot be totally explained using signal-to-noise considerations.

Another interesting feature of the coherence values is the fact that it is very nearly zero at all the harmonics of 60 Hz. During the averaging process, the coherence values for these tones decreased uniformly, while a majority of the other frequencies displayed a somewhat oscillatory nature. This unusual behavior is characteristic of two strongly uncorrelated sources of 60 Hz power. Taking many factors into account, it was determined that the two sources of 60 Hz acoustic power are the ambient intensity which was already mentioned which dominates the

## COHERENCE FUNCTION

(64 TIME-DELAYED AVERAGES)

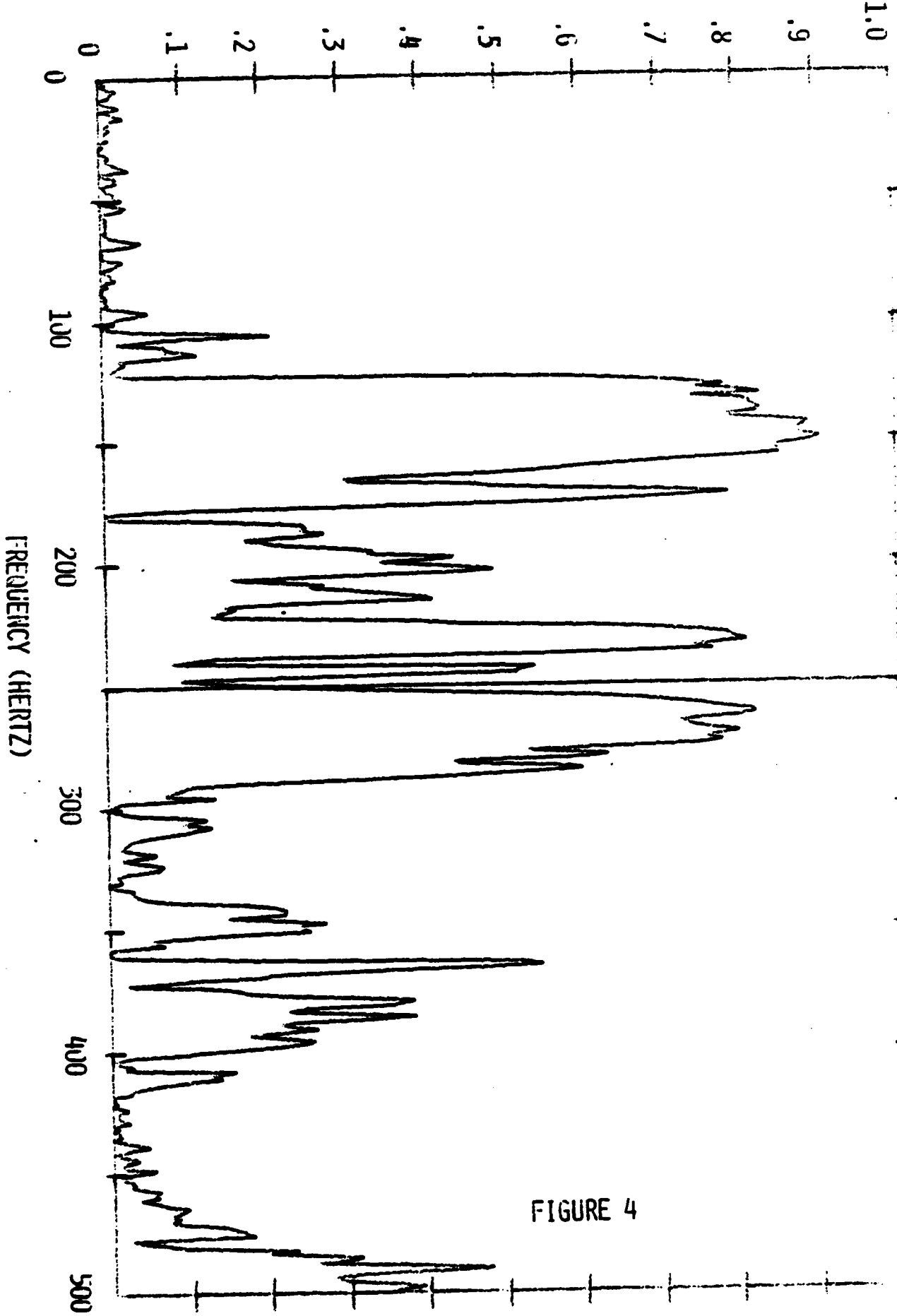


FIGURE 4

far field hydrophone, and the 60 Hz power emanating from the generator on board the YP. As expected, these two sources of 60 Hz intensity are very much uncorrelated (ie. random phase relationship), and thus produce this very low coherence.

This interesting behavior of the coherence function at 60 Hz, which was first thought to be an error in the processing, actually paved the way to the only feasible explanation for the peaks and valleys in the coherence. The valleys in the coherence function in the 120-300 Hz range can be considered analogous to the minimums at 60,120,180,...,480 Hz, there must be some source other than propeller cavitation which dominates the far field spectrum. This indicates that not all the signal-to-noise as seen in figure 3 between 120 and 300 Hz is caused by propeller noise.

To verify these hypotheses concerning the effect of propeller cavitation on the broadband vessel radiated acoustic spectra, many theoretical and experimental investigations were undertaken. As a result of this first set of data it was determined that more data should be gathered to discover the nominal value of the coherence in the given experimental environment. The puzzling problem was the fact that from a purely mathematical analysis, a signal-to-noise level of 20 dB (i.e. 150 Hz- figure 3) corresponds to a coherence of 0.99999 and from the experimental data the coherence is only 0.9 (figure 4).

#### VIII. DETERMINING THE MAXIMUM EXPECTED COHERENCE.

To determine the nominal value of the coherence, the YP was replaced by a tonal projector. Tones were examined which had high signal-to-noise in the far field, and a coherence of .9 was observed. Thus, 0.9 seems to

be the maximum coherence supportable by this acoustic environment. The same positioning of the hydrophones was used but instead of the YP, a transducer was used as the near field source of acoustic energy. The transducer was powered by a tone generator which emitted one tone every third of an octave between 20 and 500 Hz (15 tones total). Knowing the exact frequencies of these generated tones allows for the determination of characteristics of the coherence function based on these representative frequencies.

As seen from the power spectrums of the near field and the far field signals (figure 5), the tones were very much attenuated in the shallow water environment. For a few of the tones, although, enough signal-to-noise existed in the far field to yield fairly high coherence values (figure 6). Maximum values in the .8-.9 range for the 250 Hz and 490 Hz tones verify that the values gained with the YP were indeed maximums. The reason for the decrease in the signal-to-noise below approximately 100 Hz is that the cut-off frequency in the experimental environment is very near this value. The cut-off frequency is that frequency where propagation decreases rapidly on account of the waveguide properties of the surface and the bottom of the river. The reason more of the tones above 100 Hz did not yield a higher coherence is the fact that the necessary power could not be put into these tones in order to dominate the ambient noise.

A point of interest involved with the coherence function derived from this experiment is the very high coherence values at 60 Hz and its harmonics, i.e. both hydrophones are dominated by the same power cable. This result is exactly opposite the results gained from the YP data where the coherence values were very near zero. This discrepancy between the

POWER SPECTRA (TONE GENERATOR)

16 AVERAGES

dBV

26

121

111

101

91

81

NEAR FIELD

35

25

15

5

-5

0

FAR FIELD

200

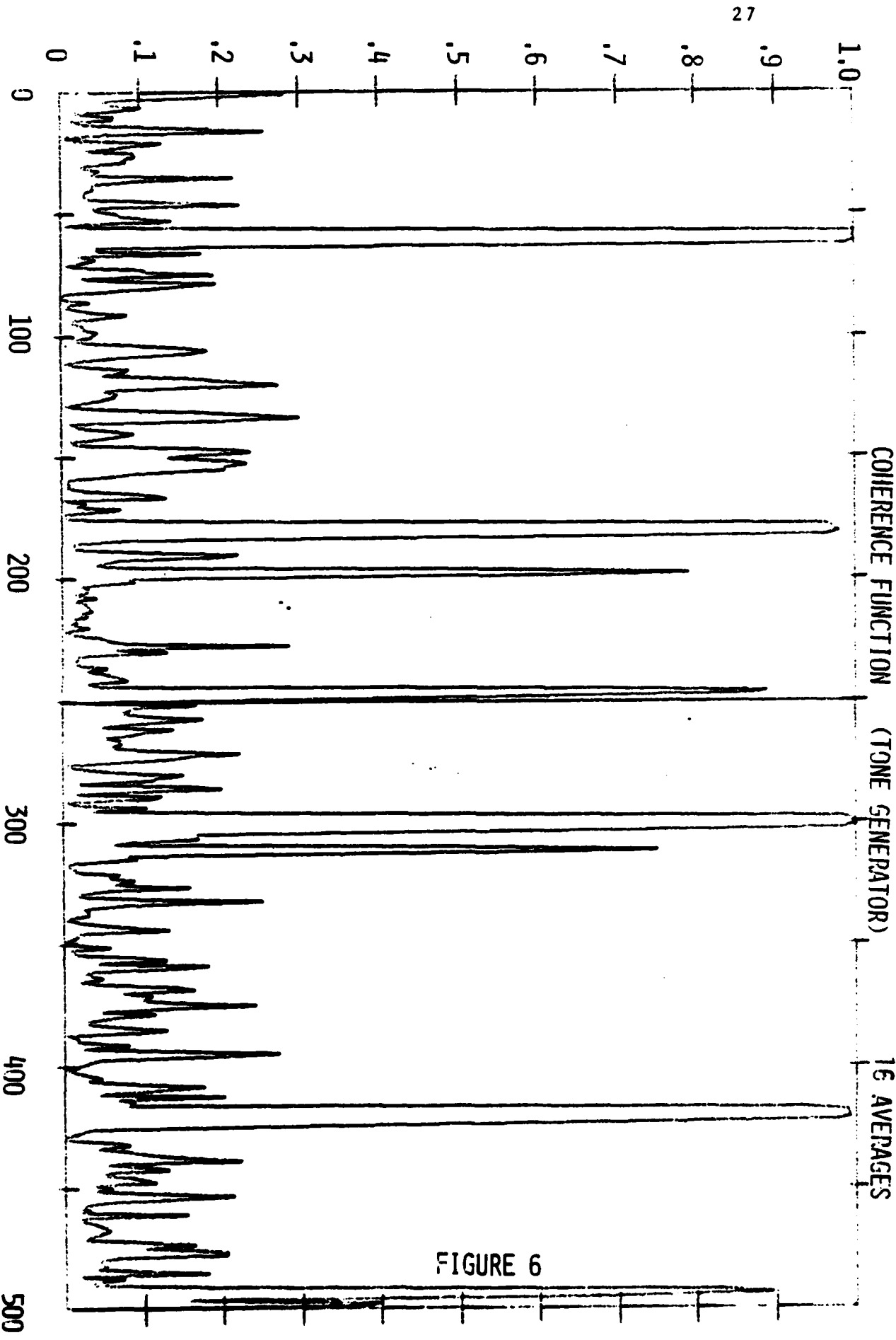
100

300

400

FREQUENCY (HERTZ)

FIGURE 5



coherence values at these frequencies actually led to the conclusion that there must be another dominant source of acoustic power on board the YP other than propeller noise, particularly sources not at the harmonics of 60 Hz. With the tone generator, a 60 Hz tone was not emitted as it was from the YP, and therefore the major source of 60 Hz power comes from the ambient noise. Since this same ambient noise energy is predominant in both the near and far field signals, the power at these frequencies should be highly coherent.

Another cross check of the coherence function was performed from the data gathered during this second experiment. Simultaneous ambient noise spectrums were taken from both near and far field hydrophones and the resulting coherence displayed minimal coherence across the frequency range (figure 7). This low coherence is expected because ambient noise is predominantly white or Gaussian noise which is always random and thus incoherent with other signal sources. The 60 Hz tone and its harmonics display high coherence in this instance as with the data gathered with the tone generator because of the coherent properties of these special frequencies in the ambient spectrum.

From this secondary experiment many useful characteristics of the coherence function have been observed. First of all, a nominal value of the coherence is approximately 0.9, so that the value gained from the YP data is indeed a maximum. Secondly, the 60 Hz coherence characteristics suggested the possibility that propeller cavitation is not the sole source of vessel radiated acoustic energy. Finally, the verification of the random properties of ambient noise were demonstrated when the two ambient time series were placed into the coherence function.

COHERENCE FUNCTION (NEAR VS FAR FIELD AMBIENT) 32 AVERAGES

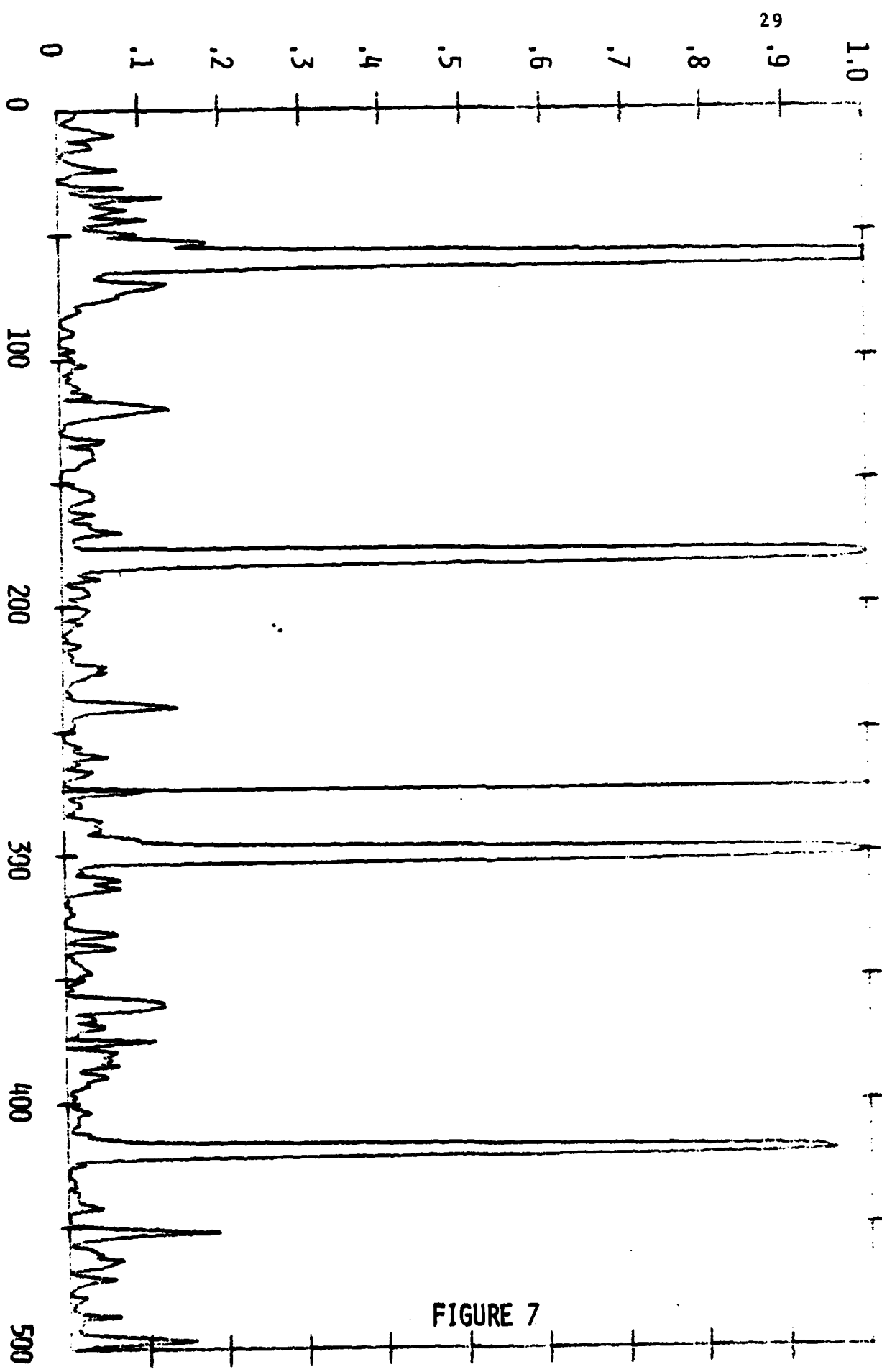


FIGURE 7

## IX. COHERENCE FUNCTION CHARACTERISTICS.

From figure 3, it can be seen that the coherence function has very abrupt discontinuities throughout the frequency range. When comparing the marked increases and decreases in the coherence values with the signal-to-noise levels (figure 2), an apparent correlation was noted between the two. From the mathematical analysis performed earlier, although, the sharp changes cannot be explained within the parameters established in the analysis. Since a purely signal-to-noise approach cannot explain the jaggedness of the coherence there must be some other cause for this behavior of the function.

Two possible explanations for this characteristic are the presence of a near field noise source or possibly the presence of far field power coming from parts of the vessel other than the propeller on board the YP. A near field noise source implies that the propeller noise is not completely dominating, and the most likely cause of this unwanted power is from flow noise around the hydrophone. A slight amount of water flow was mentioned past the stern of the YP into the propellers, so the possibility of flow noise must not be neglected. Since the deployed hydrophone displayed little deflection due to these currents, and no bubbling was observed about the hydrophone, the possibility of flow noise was not too great. To verify that flow noise actually was not a contributor to the near field signal, a mathematical treatment was undertaken.

The second and more probable cause for the jaggedness of the coherence is a source of far field power coming from sources on the YP other than the propellers. If this were the case, the signal-to-noise

levels (figure 2) would not completely represent the power in the far field emanating from the propeller which was assumed earlier. Some of the signal-to-noise level in the far field could be attributable to the diesel engines or the generator on board the YP. Naturally, power from these sources would not be coherent with the near field, propeller signal. If indeed sources other than the propellers are dominating the far field radiated spectrum, this would be contrary to the present belief that the merchant spectra is completely dominated by propeller cavitation in the far field.

The following mathematical analysis is performed to determine if enough flow noise existed in the near field to account for discontinuities in the coherence function. From the original analysis:

$$\gamma^2 = \frac{\text{INPUT POWER (in far field)}}{\text{INPUT POWER (in far field)} + \text{NOISE POWER}}$$

$$\gamma^2 = \frac{S_f^*}{S_f^* + N^*}$$

From figure 2, the signal-to-noise is 20 dB at 150 Hz, so:

Far field signal = 20 dB + ambient noise

$$S_f = 20 + N$$

The associated powers are related by:

Input power (in far field) = 100 \* Ambient noise power

$$S_f^* = 100 * N^*$$

The coherence now looks like:

$$\gamma^2 = \frac{S_f^*}{S_f^* + N^*} = \frac{100N^*}{100N^* + N^*} = \frac{100}{101} = 0.99$$

Maximum coherence!

Previously, a coherence value of 0.9 was determined to be the nominal maximum for the given experimental environment. At 150 Hz, in figure 3, the coherence is in fact 0.9, or a maximum. The mysterious feature, though, is the 0.6 drop in the coherence between 150 and 155 Hz, from 0.9 to 0.3. A signal-to-noise approach cannot explain this abrupt change:

Signal-to-noise at 155 Hz is 5 dB, or

Far field signal ( $S_f$ ) = 5 dB + Ambient Noise (N)

and, Input power ( $S_f^*$ ) =  $3.16 * \text{Noise power } (N^*)$

Finally the coherence value becomes:

$$\gamma^2 = \frac{S_f^*}{S_f^* + N^*} = \frac{(3.16)N^*}{(3.16)N^* + N^*} = \frac{3.16}{4.16} = 0.76$$

Thus, the signal-to-noise level at 155 Hz accounts for only a 0.2 drop in the coherence. The next task was to mathematically check the possibility of a flow noise contribution to the near field signal:

<u>Near field</u>	<u>Far field</u>
$x(t) + n(t)$	$y(t) = ax(t) + n(t)$
$n(t) = \text{flow noise}$	
$X(f) = R_x e^{i\phi_x} + R_{n_2} e^{i\phi_{n_1}}$	$Y(f) = aR_x e^{i\phi_x - i\omega\tau} + R_{n_2} e^{i\phi_{n_2}}$
$X(f) = S_n + N_1$	$Y(f) = S_f + N_2$

The coherence function becomes:

$$\gamma^2 = \frac{a^2 (R_x R_x^*)^2}{a^2 (R_x R_x^*) + R_x R_x^* (R_{n_2} R_{n_2}^* + a^2 R_{n_1} R_{n_1}^*) + R_{n_1} R_{n_1}^* R_{n_2} R_{n_2}^*}$$

and reduces to:

$$\gamma^2 = \frac{S_n^* S_f^*}{(S_n^* + N_1^*)(S_f^* + N_2^*)}$$

$$\gamma^2 = \frac{(\text{POWER SIGNAL-NEAR FIELD})(\text{POWER SIGNAL-FAR FIELD})}{(\text{TOTAL POWER NEAR FIELD})(\text{TOTAL POWER FAR FIELD})}$$

Fortunately, this equation reduces to the same as that derived with no flow noise when the near field signal ( $S_n^*$ ) dominates the flow noise ( $N^*$ ) and the near field terms cancel.

$$\gamma^2 = \frac{\text{POWER SIGNAL-FAR FIELD}}{\text{TOTAL POWER FAR FIELD}}$$

Just dealing with the portion of the coherence function containing the near field terms, and treating it as an adjustment factor:

$$\text{Coherence adjustment factor} = \frac{S_n^*}{S_n^* + N_l^*}$$

Using various assumed signal-to-noise levels in the near field the following table was constructed:

Signal-to-noise ratio ( $S_n - N_l$ )	Power ratio ( $S_n^*/N_l^*$ )	Coherence adjustment factor ( $S_n^*/(S_n^* + N_l^*)$ )
10 dB	10	0.91
6 dB	4	0.8
3 dB	2	0.67
0 dB	1	0.5

This adjustment factor would decrease the coherence by the calculated value if flow noise did exist in the near field. As verified above, if the near field signal is more than 10 dB above the flow noise contribution, the adjustment factor is essentially unity and has negligible effect on the coherence. Flow noise is extremely white in nature and should therefore affect all frequencies in a like manner. Consequently, the coherence adjustment factor should reduce all the coherence values the same relative amount, and thus fails to explain the 0.6 drop between 150 and 155 Hz. There is a possibility that the flow noise is highly frequency dependent, and enough of its power is concentrated at 155 Hz to account for the 0.6 drop. For this to be the case, though, the flow noise would have to completely dominate the near field propeller noise at this

frequency which is very highly unlikely with the cavitating propeller only five feet away from the hydrophone.

The discontinuous characteristics, therefore, must be explained by the presence of far field signal sources other than the propeller noise. It was this jaggedness that was first considered an experimental error which eventually substantiated the analysis of the coherence as the actual measure of the effect propeller cavitation has on the far field merchant radiated acoustic spectra. Therefore, the sharp discontinuities in the coherence indicate that sources of acoustic power from the vessel other than the propeller are dominating the far field spectra at certain frequencies. This is contrary to the present beliefs that the merchant vessel far field spectrum is totally dominated by broad-band, Gaussian, propeller cavitation.

#### X. SUMMARY OF RESULTS.

Conclusive evidence has been gained which shows that propeller cavitation is not the dominant source of acoustic energy emanating from a merchant vessel over many sonar frequency bands. Even with the YP, propeller cavitation energy did not even dominate a vessel which had no flow noise about the hull (which is a common contribution to the far field acoustic intensity). Without this flow noise, propeller cavitation would be expected to enormously overwhelm the other sources of noise onboard the vessel. At many frequencies where good signal-to-noise existed, a low coherence was gained indicating a non-propeller dominated portion of the far field spectrum. These findings about propeller cavitation energy which is propagated great distances can hopefully begin to characterize

the qualities of ambient noise in the ocean. Through this characterization, Navy sonars will be able to detect enemy targets (submarines) at much greater distances and with much greater accuracy.

The data for the YP should very nearly represent data from a standard merchant in the deep ocean. The many possible paths of propagation in the Severn River is quite similar to the numerous propagation paths in the ocean such as convergence zones and the shallow waveguide effect. Also, the YP is essentially a scaled down version of a standard merchant, a majority of oceangoing merchants now have diesel engines, highly cavitating propellers as well as electrical generators (50 Hz or 60 Hz). Considering these factors, the data and the resulting findings can be transferred to the blue-water environment of interest.

With the more complex, real-time digital spectrum analyzers being marketed today, both the quantity and quality of underwater acoustic data will be enhanced to a large extent. With the increase in precision and in speed due to these new breeds of computers, nearly all of the previously disastrous effects can be handled with relative ease. Problems such as doppler broadening, multi-path interference and precision hydrophone and projector placement can basically be eliminated via digital processing techniques. The future for underwater acoustic research looks bright, and as long as there are submarines in the oceans the Navy need will always exist. Therefore, this project answers a portion of a problem which is of importance to the Navy as well as offering an opportunity to be exposed to an exciting field of physics.

#### References

1. R.A. Wagstaff and O.Z. Bluy, "Underwater Ambient Noise Proceedings of a Conf.", Scalant ASW Research Centre, No. 32, 1979.
2. J.W. Zabalgogeazcopa, "Coherence Estimates for Signals Propagated through Acoustic Channels with Multiple Paths," *J. Acoust. Soc.*, AM72, 1982.
3. D. Ross, Mechanics of Underwater Noise, New York: Pergamon Press, 1976.
4. J.S. Bendat and A.G. Piersol, Engineering Applications of Correlation and Spectral Analysis, New York: Wiley and Sons, 1980, p. 76.

## UNCLASSIFIED

SECURITY CLASSIFICATION OF THIS PAGE (When Data Entered)

REPORT DOCUMENTATION PAGE		READ INSTRUCTIONS BEFORE COMPLETING FORM RECIPIENT'S CATALOG NUMBER
1. REPORT NUMBER U.S.N.A. - TSPR: 123 (1983)	2. GOVT ACCESSION NO. <i>A134233</i>	
4. TITLE (and Subtitle) PROPELLER CAVITATION EFFECTS ON BROADBAND VESSEL-RADIATED ACOUSTIC <i>SPECTRA</i>	5. TYPE OF REPORT & PERIOD COVERED Final: 1982/1983	
	6. PERFORMING ORG. REPORT NUMBER	
7. AUTHOR(s) Dixon, Daniel N.	8. CONTRACT OR GRANT NUMBER(s)	
9. PERFORMING ORGANIZATION NAME AND ADDRESS United States Naval Academy, Annapolis.	10. PROGRAM ELEMENT, PROJECT, TASK AREA & WORK UNIT NUMBERS	
11. CONTROLLING OFFICE NAME AND ADDRESS United States Naval Academy, Annapolis.	12. REPORT DATE 20 June 1983	
	13. NUMBER OF PAGES 37	
14. MONITORING AGENCY NAME & ADDRESS (if different from Controlling Office)	15. SECURITY CLASS. (of this report) UNCLASSIFIED	
	15a. DECLASSIFICATION/DOWNGRADING SCHEDULE	
16. DISTRIBUTION STATEMENT (of this Report) This document has been approved for public release; its distribution is UNLIMITED.		
17. DISTRIBUTION STATEMENT (of the abstract entered in Block 20, if different from Report) This document has been approved for public release; its distribution is UNLIMITED.		
18. SUPPLEMENTARY NOTES Accepted by the U. S. Trident Scholar Committee.		
19. KEY WORDS (Continue on reverse side if necessary and identify by block number) Underwater acoustics		
20. ABSTRACT (Continue on reverse side if necessary and identify by block number) To gain an understanding of ambient noise in the oceans today, the characteristics of merchant vessel acoustic spectra must be determined. Presently, it is believed that the major source of acoustic intensity emanating from a merchant ship is propeller noise. Experimental data must be gathered to verify if propeller noise is the dominating contributor to the far field radiated merchant vessel spectrum.		

(OVER)

**UNCLASSIFIED**

**SECURITY CLASSIFICATION OF THIS PAGE (When Data Entered)**

Data was gathered from a stationary vessel whose propellers are cavitating to determine exactly how much of the far field spectrum was propeller dominated. Considerations such as propagation delay and multi-path effects had to be dealt with prior to the processing procedure. Digital signal processing techniques along with the coherence function were applied to the gathered data. The resulting coherence values for frequencies of interest to Navy sonar systems (0-500 Hz) were studied and compared to the corresponding signal-to-noise level in the far field spectrum. The coherence accurately displays that, contrary to present belief, propeller cavitation is not the dominant source of merchant vessel acoustic power in the far field over the entire frequency band of interest.

S/N 0102-LF-014-6601

**UNCLASSIFIED**

**SECURITY CLASSIFICATION OF THIS PAGE(When Data Entered)**

**END**

**FILMED**

**11-83**

**DTIC**